

Synthesis of Tris(tetrathiafulvaleno)dodecadehydro- [18]annulenes and Their Self-Assembly

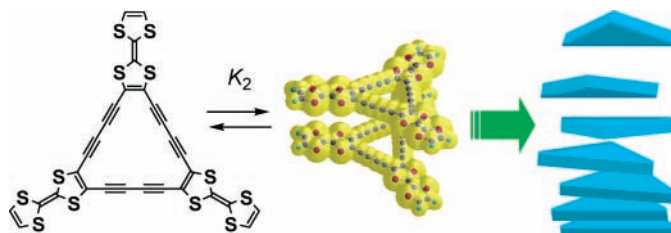
Hideo Enozawa,[†] Masashi Hasegawa,[†] Daikou Takamatsu,[‡] Ken-ichi Fukui,[‡] and Masahiko Iyoda^{*†}

Department of Chemistry, Graduate School of Science, Tokyo Metropolitan University, Hachioji, Tokyo 192-0397, Japan, and Department of Chemistry, Tokyo Institute of Technology, 2-12-1 O-okayama, Meguro-ku, Tokyo 152-8551, Japan

iyoda-masahiko@c.metro-u.ac.jp

Received March 7, 2006

ABSTRACT



Synthesis of electroactive tris(tetrathiafulvaleno)dodecadehydro[18]annulenes with ester substituents has been carried out with palladium-mediated cyclotrimerization of 4,5-diethynyl-TTFs. The TTF[18]annulenes produce stacked dimers in solution and exhibit solvatochromism and thermochromism. The TTF[18]annulene-hexabutyl ester forms a molecular wire from an aqueous THF solution with cooperative S–S and π – π stacking interactions.

Self-assembly of conjugated macrocycles¹ and long helical molecules² into complex, organized supramolecular structures via specific intermolecular interactions is a promising way to realize new molecular materials.³ Many intermolecular

interactions such as hydrogen bonding,⁴ metal coordination,⁵ CT interaction,⁶ and π stacking⁷ have been utilized recently to construct desired supramolecular architectures. Among these, cooperative S–S and π – π stacking interactions of

[†] Tokyo Metropolitan University.

[‡] Tokyo Institute of Technology.

(1) (a) Höger, S. In *Acetylene Chemistry: Shape-Persistent Macrocycles for Ordered Systems*; Diederich, F., Stang, P. J., Tykwinski, R. R., Eds.; Wiley-VCH: Weinheim, Germany, 2005. (b) Höger, S. *Chem. Eur. J.* **2004**, *10*, 1320–1329. (c) Zhao, D. H.; Moore, J. S. *Chem. Commun.* **2003**, 807–818. (d) Yamaguchi, Y.; Yoshida, Z. *Chem. Eur. J.* **2003**, *9*, 5430–5440. (e) Bunz, U. H. F.; Rubin, Y.; Tobe, Y. *Chem. Soc. Rev.* **1999**, *28*, 107–119.

(2) (a) Ray, C. R.; Moore, J. S. *Adv. Polym. Sci.* **2005**, *177*, 91–149. (b) Stone, M. T.; Moore, J. S. *J. Am. Chem. Soc.* **2005**, *127*, 5828–5935. (c) Tanaka, Y.; Katagiri, H.; Furusho, Y.; Yashima, E. *Angew. Chem., Int. Ed.* **2005**, *44*, 3867–3870. (d) Inouye, M.; Waki, M.; Hajime, A. *J. Am. Chem. Soc.* **2004**, *126*, 2022–2027.

(3) (a) *Molecular Switches*; Feringa, B. L., Ed.; Wiley-VCH: Weinheim, Germany, 2001. (b) *Molecular Devices and Machines*; Balzani, V., Venturi, M., Credi, A., Eds.; Wiley-VCH: Weinheim, Germany, 2003. (c) Benniston, A. C. *Chem. Soc. Rev.* **2004**, *33*, 573–578. (d) Wouters, D.; Schubert, U. S. *Angew. Chem., Int. Ed.* **2004**, *43*, 2480–2495. (e) Wassel, R. A.; Gorman, C. B. *Angew. Chem., Int. Ed.* **2004**, *43*, 5120–5123.

(4) (a) Jørgensen, M.; Bechgaard, K.; Bjørnholm, T.; Sommer-Laesen, P.; Hansen, L. G.; Schaumburg, K. *J. Org. Chem.* **1994**, *59*, 5877–5882. (b) Gall, T. L.; Pearson, C.; Bryce, M. R.; Petty, M. C.; Dahlgard, H.; Becher, J. *Eur. J. Org. Chem.* **2003**, 3562–3568. (c) Bushey, M. L.; Nguyen, T.-Q.; Zhang, W.; Horoszewski, D.; Nuckolls, C. *Angew. Chem., Int. Ed.* **2004**, *43*, 5446–5453. (d) Brammer, L. *Chem. Soc. Rev.* **2004**, *33*, 476–489. (e) Huc, I. *Eur. J. Org. Chem.* **2004**, 17–29.

(5) (a) Ruben, M.; Rojo, J.; Romero-Salguero, F. J.; Uppadine, L. H.; Lehn, J.-L. *Angew. Chem., Int. Ed.* **2004**, *43*, 3644–3662. (b) Kitagawa, S.; Kitaura, R.; Noro, S. *Angew. Chem., Int. Ed.* **2004**, *43*, 2334–2375. (c) Hofmeier, H.; Schubert, U. S. *Chem. Soc. Rev.* **2004**, *33*, 373–399. (d) Würthner, F.; You, C.-C.; Saha-Möller, C. R. *Chem. Soc. Rev.* **2004**, *33*, 133–146. (e) Oh, M.; Carpenter, G. B.; Sweigart, D. A. *Acc. Chem. Res.* **2004**, *37*, 1–11.

(6) (a) Marsden, J. A.; Miller, J. J.; Shirtcliff, L. D.; Haley, M. M. *J. Am. Chem. Soc.* **2005**, *127*, 2464–2476. (b) Pease, A. R.; Jeppesen, J. O.; Stoddart, J. F.; Luo, Y.; Collier, C. P.; Heath, J. R. *Acc. Chem. Res.* **2001**, *34*, 433–444.

(7) Watson, M. D.; Fechtenkotter, A.; Müllen, K. *Chem. Rev.* **2001**, *101*, 1267–1300.

oligomeric tetrathiafulvalenes (TTFs) can play an important part in preparing columnar aggregates with high charge carrier mobilities. Quite recently, several groups independently reported the formation of molecular wires containing TTF segments of self-assembling systems.^{8,9} These self-assembled materials having TTF moieties have been designed as gelators which require hydrogen bonding sites⁹ or crown ether substructures.⁸ To make self-assembled materials based on fully conjugated oligomeric TTFs^{10,11} with potential conducting and magnetic properties, we designed tris-(tetrathiafulvaleno)dodecahydro[18]annulenes (**1a** and **1b**) composed of a large TTF-annulene core, ester groups, and peripheral alkyl chains (Figure 1). We report here the

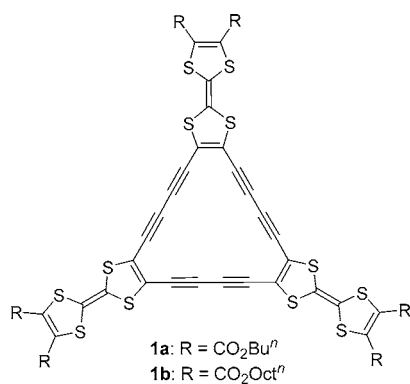
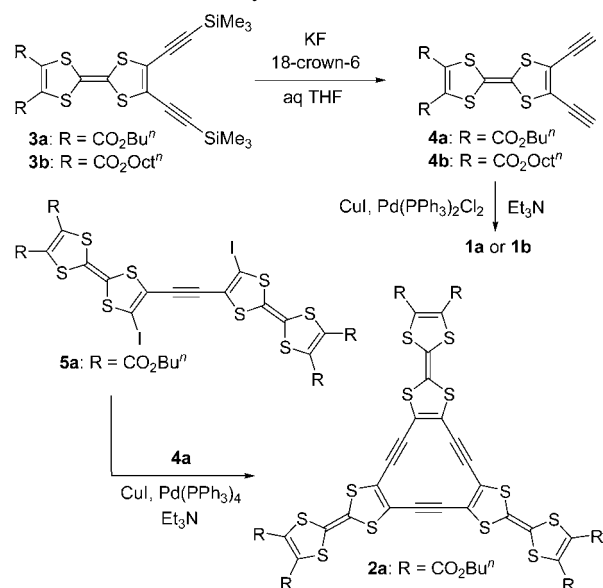


Figure 1. TTF[18]annulenes **1a** and **1b**.

synthesis of **1a,b** and their solvatochromic and thermochromic properties mainly caused by self-assembly of **1a,b** in solution, and the formation of molecular wire from an aqueous THF solution of **1a**, together with the synthesis and properties of the analogous TTF[12]annulene **2a**.

Syntheses of **1a**, **1b**, and **2a** were carried out by using the sequence outlined in Scheme 1. Bis(trimethylsilylethynyl)-TTFs **3a** and **3b** have been prepared from the corresponding diiodo TTFs. Removal of the trimethylsilyl groups in **3a** and **3b** with KF and 18-crown-6 in aqueous THF forms unstable **4a** and **4b** in quantitative yields. The palladium-mediated

Scheme 1. Syntheses of **1a**, **1b**, and **2a**



coupling of **4a** and **4b** in THF in the presence of CuI and Et₃N produced **1a** and **1b** in 29% and 33% yields based on **3a** and **3b**, respectively. To compare the association properties, the corresponding TTF[12]annulene **2a** also has been synthesized in 25% yield via a modification of a reported procedure.¹² The TTF[18]annulenes **1a** and **1b** are fairly stable at ambient temperature under air, whereas the TTF[12]annulene **2a** decomposes gradually under the same conditions.

STM measurements of **1a** and **1b** were performed to confirm the size and shape of the synthesized molecules. A dilute solution of **1a** or **1b** in CH₂Cl₂ was deposited on a Au(111) surface to obtain well-dispersed molecules. As for **1a**, each molecule is imaged as a rounded triangle ca. 2.2 nm long, with an apparent height of 0.2–0.25 nm (Figure S10, Supporting Information). A comparison of the image with a molecular model suggests that the major contribution for the electron tunneling seems to originate from π states of annulene as well as the TTF moiety formed above the Fermi level as a result of interaction with the Au surface. The STM image of **1b** supports this assignment because a single **1b** molecule showed a similar size to **1a** (Figure S11, Supporting Information).¹³

Although **1a,b** and **2a** show no self-aggregation in CDCl₃, CD₂Cl₂, or THF-*d*₈, these compounds aggregate strongly in benzene and toluene. The dimerization constants were determined by curve fitting of the concentration- and temperature-dependent ¹H NMR data of **1a,b** and **2a**, together with vapor pressure osmometric (VPO) measurements. Interestingly, **1a** exhibits a bigger *K*₂ value than **2a** (Table

(8) (a) Sly, J.; Kasák, P.; Gomar-Nadal, E.; Rovira, C.; Górriz, L.; Thorarson, P.; Amabilino, D. B.; Rowan, A. E.; Nolte, R. J. M. *Chem. Commun.* **2005**, 1255–1257. (b) Akutagawa, T.; Kakiuchi, K.; Hasegawa, T.; Noro, S.; Nakamura, T.; Hasegawa, H.; Mashiko, S.; Becher, J. *Angew. Chem., Int. Ed.* **2005**, *44*, 7283–7287.

(9) (a) Kitamura, T.; Nakaso, S.; Mizoshita, N.; Tochigi, Y.; Shimomura, T.; Moriyama, M.; Ito, K.; Kato, T. *J. Am. Chem. Soc.* **2005**, *127*, 14769–14775. (b) Kitahara, T.; Shirakawa, M.; Kawano, S.; Beginn, U.; Fujita, N.; Shinkai, S. *J. Am. Chem. Soc.* **2005**, *127*, 14980–14981. (c) Wang, C.; Zhang, D.; Zhu, D. *J. Am. Chem. Soc.* **2005**, *127*, 16372–16373.

(10) (a) Iyoda, M.; Hasegawa, M.; Miyake, Y. *Chem. Rev.* **2004**, *104*, 4887–5782. (b) Iyoda, M. In *TTF Chemistry*; Yamada, T., Sugimoto, T., Eds.; Kodansha & Springer-Verlag: Tokyo, Japan, 2004; Chapter 8.

(11) (a) Hasegawa, M.; Takano, J.; Enozawa, H.; Kuwatani, Y.; Iyoda, M. *Tetrahedron Lett.* **2004**, *45*, 4109–4112. (b) Becher, J.; Brimert, T.; Jeppesen, J. O.; Pedersen, J. Z.; Zubarev, R.; Bjørnholm, T.; Reitzel, N.; Jensen, T. R.; Kjaer, K.; Levillain, E. *Angew. Chem., Int. Ed.* **2001**, *40*, 2497–2500. (c) Godbert, N.; Batsanov, A. S.; Bryce, M. R.; Howard, J. A. K. *J. Org. Chem.* **2001**, *66*, 713–719. (d) Derf, F. L.; Levillain, E.; Trippé, G.; Gorgues, A.; Sallé, M.; Sebastián, R.-M.; Caminade, A.-M.; Majoral, J.-P. *Angew. Chem., Int. Ed.* **2001**, *40*, 224–227.

(12) (a) Hara, K.; Hasegawa, H.; Kuwatani, Y.; Enozawa, H.; Iyoda, M. *Chem. Commun.* **2004**, 2042–2043. (b) Iyoda, M.; Enozawa, H.; Miyake, Y. *Chem. Lett.* **2004**, *33*, 1098–1099.

(13) STM measurements of **1a** and **1b** were performed in ambient air at room temperature with mechanically cut Pt/Ir tips. See the Supporting Information.

1). The TTF[18]annulene **1a** has smaller ΔH and ΔS values

Table 1. Association Constants and Thermodynamic Parameters for Dimerization of **1a**, **1b**, and **2a** in Toluene- d_8

compd	K_2 (M^{-1}) ^a	ΔG ($kJ \cdot mol^{-1}$) ^a	ΔH ($kJ \cdot mol^{-1}$)	ΔS ($J \cdot mol^{-1} \cdot K^{-1}$)
1a	522 ± 50	-15.2	-37.7	-76.9
1b	543 ± 67	-15.3	-46.3	-105
2a	176 ± 8.0	-12.6	-32.0	-66.3

^a At 293 K.

than the TTF[12]annulene **2a**, suggesting higher stacking ability and a larger ring size for **1a**. Furthermore, the much smaller ΔH and ΔS values for **1b** as compared to **1a** indicate the stronger solvophobic effect and larger molecular size of **1b** owing to longer alkyl substituents because alkyl-alkyl interaction dominates over alkyl-benzene (toluene) interaction. Although the electronic spectra of **1a** in benzene and toluene show no concentration dependence due to the low content of the dimer in a dilute solution at room temperature (ca. 5% of the dimer is formed in a 1×10^{-4} M solution of **1a** in benzene), a film of **1a** prepared from a benzene solution exhibits a red shift (from 505 to 540 nm) of the longest absorption maximum with a color change from red to violet, presumably due to the formation of the dimer or higher aggregates. Similarly, **1b** shows a color change from red to violet and a red shift of the longest absorption maximum from 506 nm (benzene) (toluene) solution to 530 nm (film). Furthermore, **1a** and **1b** show thermochromism (Figure 2).

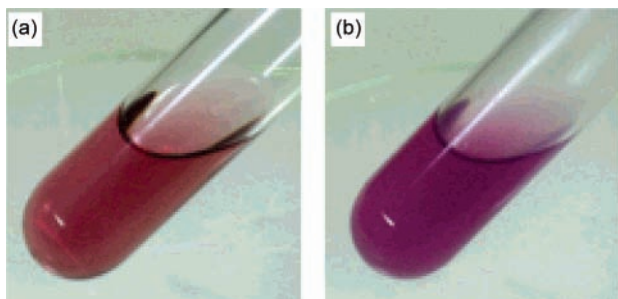


Figure 2. Colors of a solution of **1a** in toluene (2.5×10^{-5} M) at room temperature (a) and at -78 °C (b).

Thus, the color of dilute solutions (10^{-4} – 10^{-5} M) of **1a** and **1b** in toluene changes from red at room temperature to violet at -78 °C, and the wavelengths of absorption maxima also shift from 509 nm at 20 °C to 525 nm at -80 °C for **1a** (2.12×10^{-4} M) and from 508 nm at 20 °C to 529 nm at -80 °C for **1b** (2.06×10^{-4} M). In these temperature ranges and concentrations, a drastic change of the monomer/dimer ratio for **1a** and **1b** is evidenced by the thermodynamic parameters shown in Table 1 [monomer/dimer = 98/2 at room temperature and monomer/dimer = 12/88 at -78 °C

based on the dimer model for **1a**] (see the Supporting Information).

Since **1a,b** and **2a** show aggregation properties in a suitable solvent, it should be possible to construct a giant-sized molecular wire from solution states via self-assembly. To confirm this, water was added to a solution of **1a** in THF to prepare a 1:1 mixed solvent of THF and H_2O . Although no gelation was observed, the color of the solution (3.04×10^{-4} M) suddenly changed from red to violet, and the absorption maximum shifted from 498 to 519 nm, indicating the formation of higher aggregates (Figure 3).¹⁴ After the

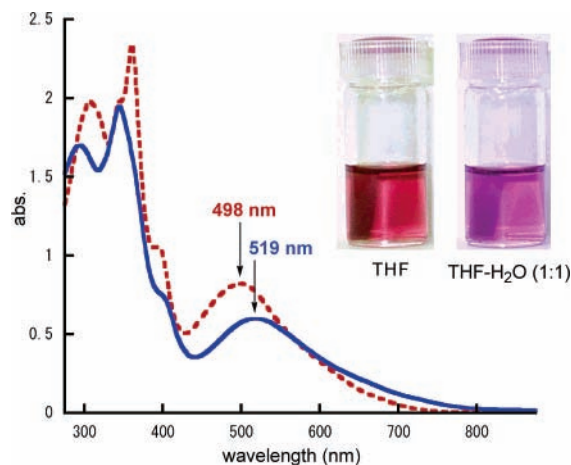


Figure 3. Electronic spectra of solutions of **1a** (3.04×10^{-5} M) in THF (dotted red line) and THF- H_2O (1:1) (solid blue line).

solution was left standing at room temperature for a few hours, the absorption spectrum gradually changed (from 519 to 558 nm; Figure S19, Supporting Information) and a stringy violet material was formed (Figure 4a). Interestingly, the stringy material formed a fibrous superstructure after standing on a glass plate at room temperature under air (Figure 4b). As shown in Figure 4c, the dried material exhibits a marked fibrous structure 50–500 nm thick. This fibrous material is readily soluble in THF, and the starting **1a** can be recovered without decomposition. Taking into account the molecular size, 500–1000 strands of the stacked molecular wire of **1a** form the semimicron-size fibrous structure.

In contrast to the molecular wire formation of **1a**, the hexaester **1b** with longer alkyl chains shows a different behavior. When water was added to a solution of **1b** (1.83×10^{-5} M) in THF, the color of the THF- H_2O (1:1) solution changed from red to violet, and the absorption maximum shifted from 498 to 517 nm in analogy with **1a** (Figure S20, Supporting Information). However, no precipitate or wire was formed on standing at room temperature or at 0 °C for

(14) As shown in Figure 3, **1a** has two absorption bands at ca. 350 nm and ca. 500 nm due to π - π^* and CT absorptions, respectively. The CT absorption band based on the donor (TTF) and acceptor (annulene) system shows a red shift through aggregation (**1a**: 498 to 519 nm in THF- H_2O), whereas π - π^* absorption exhibits a blue shift through aggregation (**1a**: 360 to 344 nm in THF- H_2O).

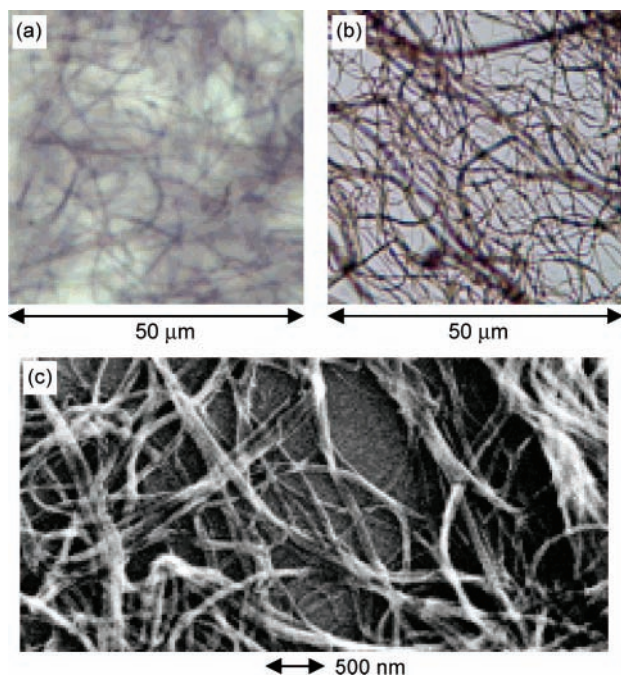


Figure 4. Microscopic images of **1a**. Optical micrographs on a glass plate from a microscope with 1000 \times magnification: (a) stringy material formed in aqueous THF solution; (b) fibrous structure obtained by drying **1a** threads on a silicon wafer. (c) SEM picture of **1a** threads on a silicon wafer.

several days. A more concentrated solution of **1b** ($\sim 10^{-3}$ M) in THF–H₂O (1:1) gave a colloidal solution, but no wire formation was also observed. The difference in aggregation behavior between **1a** and **1b** may depend on their different solubilities and thermodynamic parameters ΔH and ΔS .

The TTF[18]annulenes **1a,b** and the TTF[12]annulene **2a** are multiredox systems with donor–acceptor combination. Thus, **1a** exhibits two oxidation potentials in dilute solution (1.22×10^{-4} M) [**1a**: $E^{\text{ox}1}_{1/2} = 0.43$ (broad), $E^{\text{ox}2}_{1/2} = 0.70$ V, vs Fc/Fc⁺ in CH₂Cl₂], indicating formation of the cation radical **1a**^{3(•+)} and the dication **1a**³⁽²⁺⁾. In contrast, **2a** shows three oxidation potentials in dilute solution (1.28×10^{-4} M) [**2a**: $E^{\text{ox}1}_{1/2} = 0.29$, $E^{\text{ox}2}_{1/2} = 0.44$ (broad), $E^{\text{ox}3}_{1/2} = 0.66$ V, vs Fc/Fc⁺ in CH₂Cl₂], suggesting formation of the corresponding cation radicals **2a**^{•+}, **2a**²⁺, and **2a**³⁺ and the dication

2a³⁽²⁺⁾ due to intramolecular and intermolecular interactions.¹⁵ Although **2a** exhibits two reversible one-electron reductions based on the formation of the stable 14 π -electron dianion, **1a,b** exhibit only one irreversible reduction process. Doping of iodine vapor into compressed pellets of **1a,b** and **2a** produced black cation radical salts which showed electric conductivities of 2.4×10^{-2} , 5.6×10^{-3} , and 4.3×10^{-3} S \cdot cm⁻¹, respectively.¹⁶

In summary, redox-active nanoscale aggregates of tris-(tetrathiafulvaleno)dodecahydro[18]annulenes **1a** and **1b** have been constructed in solution, and the aggregation behavior of **1a** and **1b** has been directly correlated with their solvatochromism and thermochromism. Furthermore, a fibrous structure of the nanoaggregates of **1a** is visualized with use of an optical microscope and a SEM micrograph. Stacking and electroconductive properties of TTF units in **1a,b** and **2a** are utilized for formation of semiconductors through iodine doping. These nanoaggregates based on TTF trimers open up interesting perspectives in the field of molecular switches, devices, and machines in nanotechnology and electronic applications.

Acknowledgment. This work was supported by a Grant-in-Aid for Scientific Research from the Ministry of Education, Culture, Sports, Science, and Technology, Japan. The authors are grateful to Prof. Y. Tobe (Osaka University) for the VPO measurements and to Dr. K. Hara, Dr. Y. Miyake, Dr. Y. Kuwatani, Dr. T. Nishinaga, Mr. M. Kakuta, and Miss Y. Nakajima (Tokyo Metropolitan University) for experimental assistance.

Supporting Information Available: Synthetic procedures and additional characterization data. This material is available free of charge via the Internet at <http://pubs.acs.org>.

OL0605530

(15) The redox waves and potentials of **1a,b** and **2a** measured by cyclic voltammetry are solvent and concentration dependent, reflecting the intramolecular and intermolecular interactions of intermediately formed cationic species. See the Supporting Information.

(16) Doping of iodine vapor was carried out by using a compressed pellet of ca. $1 \times 0.5 \times 0.01$ mm³ size, to which two gold wires were attached apart by ca. 0.5 mm. Before doping, each sample prepared from **1a,b** and **2a** was an insulator. After doping of iodine vapor for 5–70 min, however, each sample showed the maximum electric conductivity, and then the conductivity was reduced gradually to less than one-half of its maximum value. The maximum conductivities in all cases were reported in the text.